(C(5)) in Cu(hyxan)SO_4·2H_2O and 0.011 Å (N(7)) in the respective cadmium compound. The extraannular oxygen atom O(6) lies 0.050 Å below (Cu) or 0.029 Å above (Cd) this purine plane.

Purine Stacking and Hydrogen Bonding. A packing diagram of the structure of M(hyxan)SO_4·2H_2O is presented in Figure 3. On the basis of the classification proposed by Bugg,[31] a solid-state stacking pattern of the purine rings of type II occurs, where the stacking bases are rotated approximately 180° with respect to each other. In M(hyxan)SO_4·2H_2O, the stacking base pairs are related by a center of inversion and therefore are exactly parallel by crystallographic symmetry. The stacking involves interactions of the polar carbonyl groups with the imidazole rings of adjacent purines, but there is only minor direct overlap because the rings are not perpendicular in relation to their translation axis. The stacking distances between hypoxanthine bases, calculated as the mean distance of all atoms of one molecule from the least-squares plane through the stacking molecule is 3.30 Å in Cu(hyxan)-SO_4·2H_2O and 3.34 Å in Cd(hyxan)SO_4·2H_2O.

A summary of hydrogen-bonded contacts and their geometry is presented in Table IX. The coordinating hypoxanthine molecules are involved in three hydrogen bonds of the type N-H···O with a bifurcated hydrogen-bonding system around H(1). As mentioned above, the bridging water molecule is involved in strong hydrogen bonds with a minimum O···O donor-acceptor distance of 2.57 Å (Cu) and 2.62 Å (Cd), respectively. The nonbridging water molecule exhibits hydrogen bonds with corresponding minimum O···O distances of 2.77 Å (Cu) and 2.76 Å (Cd), respectively.

Acknowledgment. We thank Professor H. R. Oswald for standing support of this project. Research grants from the Swiss National Science Foundation (No. 2.838-085) are gratefully acknowledged.

Supplementary Material Available: Tables listing details of data collection and structure refinement, anisotropic thermal parameters, and bonding distances and angles involving H atoms for the two structures (4 pages); listings of observed and calculated structure factors (32 pages). Ordering information is given in any current masthead page.

(31) Bugg, C. E. *The Jerusalem Symposia on Quantum Chemistry and Biochemistry*; Jerusalem Academy of Sciences and Humanities: Jerusalem, 1972; Vol 4., p 178.

Contribution from the Chemistry Department,
The Ohio State University, Columbus, Ohio 43210

Synthesis and Structural Characterization of a Neutral Lacunar Complex Formed by Deprotonation of Methyl Groups of the Cyclidene Macrocycle

Kenneth A. Goldsby, Alan J. Jircitano, Dennis L. Nosco, James C. Stevens, and Daryle H. Busch*

Received July 7, 1989

X-ray structural analysis, electrochemistry, and reactivity with dioxygen are reported for the complex [Co{$(CH_2)_2(MeN)_2(CH_2)_6$[16]cyclidene}]. The neutral complex is formed by deprotonation of the parent $(CH_2)_6$-bridged lacunar cyclidene complex. The structural differences between the parent and deprotonated complexes can be understood in terms of the redistribution of electron density upon deprotonation. The centralization of electron density and reduction in charge concomitant with deprotonation result in a large cathodic shift for the potential required to oxidize the cobalt(II) and structurally analogous nickel(II) complexes. The neutral cobalt(II) complex autoxidizes much faster than the corresponding cationic parent complex, and this has prevented dioxygen affinity measurements. [CO{$(CH_2)_2(MeN)_2(CH_2)_6$[16]cyclidene}] crystallized in the monoclinic system ($P2_1/n$) with unit cell dimensions a = 13.824 (2) Å, b = 11.351 (2) Å, c = 17.852 (2) Å, β = 115.16 (1)°, and Z = 4; R = 0.064 and R_w = 0.073 for 2666 observed reflections.

Introduction

A major focus of our work has involved the design and synthesis of a new family of lacunar (structure I) and vaulted (structure II) complexes capable of binding small molecules and/or organic substrates.[1,2] These complexes are based on the parent cyclidene

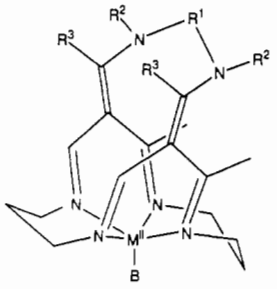

I

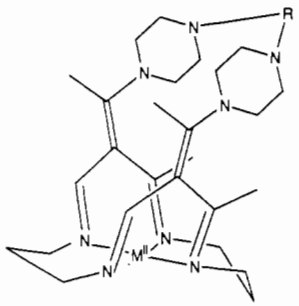

II

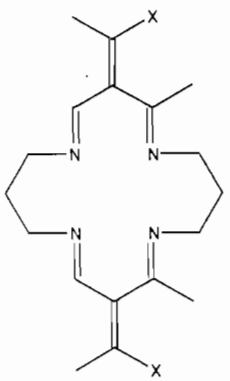

(X = OR, NRR^1)

III

macrocycle shown in structure III. The cyclidene macrocycle is particularly amenable to these studies, since the ligand superstructure may be easily modified to control the shape and size of the substrate binding site.[1-5]

In the course of developing the synthetic methodology used to modify the cyclidene macrocycle, we have explored the depro-

* To whom correspondence should be addressed at the Chemistry Department, The University of Kansas, Lawrence, KS 66045-0046.

(1) (a) Cairns, C. J.; Busch, D. H. *Progress in Macrocycle Chemistry*; Izatt, R. N., Christensen, J. J., Eds.; Wiley-Interscience: New York, 1987; pp 1-51. (b) Busch, D. H. *Oxygen Complexes and Oxygen Activation*; Martell, A. E., Sawyer, D. T., Eds.; Plenum Publ. Co.: New York, 1988; pp 61-85.

0020-1669/90/1329-2523$02.50/0

tonation reactions of these complexes. When R^2 (or R^1) = H, then deprotonation at both sites gives dinucleophiles, which upon reaction with alkyl halides form N–C bonds.[3-5] In fact, the deprotonation of unbridged precursors has been used in the synthesis of some of the lacunar cyclidene complexes.[3-5] If R^2 (and R^1) ≠ H and R^3 = Me, then deprotonation will occur at the R^3 methyl sites to give neutral complexes of the kind shown in structure IV.[3] Regardless of the site of deprotonation, the net results are to (1) lower the charge of the complex by two electrostatic units, and (2) redistribute the electron density more in the vicinity of the metal ion.

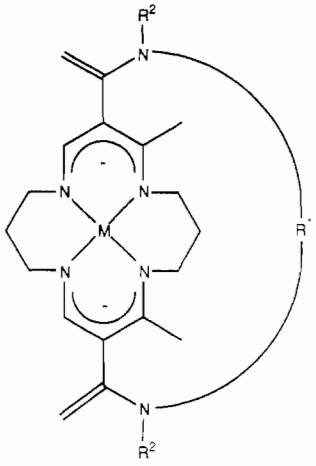

IV

The concomitant reduction in charge and centralization of electron density associated with deprotonation are expected to alter the structure and redox properties of the cyclidene complexes, both of which are important considerations in designing host molecules for inclusion complexes. As such, these relatively stable nucleophiles are themselves worthy of study.

With this objective in mind, we have synthesized and structurally characterized the deprotonated lacunar cyclidene complex [Co{$(CH_2)_2(MeN)_2(CH_2)_6$[16]cyclidene}] (structure IV, where M = Co, R^2 = Me, and $R^1 = (CH_2)_6$). This complex is particularly desirable in that direct comparison can be made between it and the parent $(CH_2)_6$-bridged cobalt(II) lacunar complex, the structure of which has been reported.[6] The reactivity with dioxygen is of special interest, since the neutral deprotonated complex electronically resembles the synthetic porphyrin[7] and Schiff base[8] cobalt(II) dioxygen carriers. Therefore, the reactivity of [Co{$(CH_2)_2(MeN)_2(CH_2)_6$[16]cyclidene}] with dioxygen has been investigated, and this too can be compared with the known dioxygen-binding behavior of the lacunar cyclidene cobalt(II) complexes, particularly the parent $(CH_2)_6$-bridged complex.[9-11]

Table I. Crystal Data for [Co{$(CH_2)_2(MeN)_2(CH_2)_6$[16]cyclidene}]

chem formula	$CoC_{26}H_{40}N_6$	fw	495.59
a	13.824 (2) Å	space group	$P2_1/n$
b	11.351 (2) Å	T	20 °C
c	17.852 (2) Å	ρ_{calcd}	1.298 g cm^{-3}
β	115.16 (1)°	$\mu_{Mo K\alpha}$	7.31 cm^{-1}
V	2535 (11) Å^3	$R(F_o)$	0.064
Z	4	$R_w(F_o)$	0.073

As expected, the potential for oxidation of the $(CH_2)_6$-bridged cobalt(II) lacunar complex shows a cathodic shift upon deprotonation. The difference in potentials for oxidation of the deprotonated and parent cobalt(II) complexes is quite large (ca. 0.7 V), especially given that deprotonation occurs at a carbon atom five bonds from the metal center. The analogous nickel(II) cyclidene complexes show a similar shift, and the potentials may offer some insight into the site of oxidation for the deprotonated cyclidene complexes.

Experimental Section

Materials. Reagent grade solvents and chemicals were used in the synthesis of the nickel(II) and cobalt(II) complexes. Solvents were dried following recommended procedures[12] and distilled under nitrogen before use. Electrochemical grade tetra-*n*-butylammonium tetrafluoroborate (TBAT) was purchased from Southwestern Analytical Co. and used as received.

Synthesis. The complexes [Ni{$(CH_3)_2(MeN)_2(CH_2)_6$[16]cyclidene}]$(PF_6)_2$[3] and [Co{$(CH_3)_2(MeN)_2(CH_2)_6$[16]cyclidene}]$(PF_6)_2$[13] were prepared according to published procedures.

(2,11-Dimethylidene-3,10,20,26-tetramethyl-3,10,14,18,21,25-hexaazabicyclo[10.7.7]hexacosa-13,19,20,26-tetraeneato-κ^4N)nickel(II), [Ni{$(CH_2)_2(MeN)_2(CH_2)_6$[16]cyclidene}]. As reported earlier, this compound was prepared from [Ni{$(CH_3)_2(MeN)_2(CH_2)_6$[16]cyclidene}]$(PF_6)_2$ (4.21 g) by reaction with sodium methoxide in acetonitrile.[14]

(2,11-Dimethylidene-3,10,20,26-tetramethyl-3,10,14,18,21,25-hexaazabicyclo[10.7.7]hexacosa-13,19,20,26-tetraeneato-κ^4N)cobalt(II), [Co{$(CH_2)_2(MeN)_2(CH_2)_6$[16]cyclidene}]. A solution of excess sodium methoxide (freshly prepared as described above) was added to 2.0 g (2.5 mmol) of [Co{$(CH_3)_2(MeN)_2(CH_2)_6$[16]cyclidene}]$(PF_6)_2$ dissolved in 10 mL of acetonitrile, giving a deep purple solution. The solvent was removed under vacuum, and 50 mL of xylene was added to the residue. The mixture was heated at reflux, filtered through Celite, and allowed to cool, yielding the purple product. Yield: 0.65 g (56%). Anal. Calcd for $C_{26}H_{42}N_6Co$: C, 62.76; H, 8.51; N, 16.89; Co, 11.84. Found: C, 62.85; H, 8.70; N, 16.77; Co, 11.73.

Physical Measurements. Electrochemical measurements were performed by using a Princeton Applied Research Model 173 potentiostat equipped with a Model 175 linear programmer. Current vs potential curves were measured on a Houston Instruments Model 2000 XY recorder. Measurements were carried out at a platinum disk in 0.2 M TBAT/CH_2Cl_2, and the potentials were referenced to the ferrocene/ferrocenium couple.[15] Half-wave potentials were determined as the average of the peak cathodic and peak anodic potentials; i.e. $E_{1/2} = (E_{p,a} + E_{p,c})/2$. All measurements for the cobalt(II) complexes were performed in a glovebox under an atmosphere of dry nitrogen.

Elemental analyses were performed by Galbraith, Inc., Knoxville, TN.

Crystal Data. Data were collected with a Syntex $P2_1$ four-circle automated diffractometer using graphite-monochromated Mo Kα radiation. Crystals were grown by slow evaporation from acetonitrile as dark purple blocks. A crystal was mounted inside a 0.7 mm diameter capillary tube and glued with epoxy. Crystal data information is given in Table I. Preliminary measurements indicated monoclinic symmetry with systematic absences $h0l$, $h + l = 2n + 1$, and $0k0$, $k = 2n + 1$, indicative of space group $P2_1/n$. Unit cell parameters were determined by accurate centering of 15 reflections well-distributed in reciprocal space. Data were collected by using the θ–2θ technique, with a variable scan rate ranging from 2.0 to 24.0°/min in the region $4° < 2\theta < 50°$, depending upon the intensity of a 2-s prescan. The scan range was 1.0° below the Kα_1 peak to 1.0° above Kα_2, with background counts taken with a background-

(2) (a) Meade, T. J.; Busch, D. H. *Prog. Inorg. Chem.* **1985**, *33*, 59. (b) Busch, D. H. *Tranfus. Sangue* **1988**, *33*, 57.
(3) Busch, D. H.; Olszanski, D. J.; Stevens, J. C.; Schammel, W. P.; Kojima, M.; Herron, N.; Zimmer, L. L.; Holter, K. A.; Mocak, J. *J. Am. Chem. Soc.* **1981**, *103*, 1478.
(4) Busch, D. H.; Jackels, S. C.; Callahan, R. W.; Grzybowski, J. J.; Zimmer, L. L.; Kojima, M.; Olszanski, D. J.; Schammel, W. P.; Stevens, J. C.; Holter, K. A.; Mocak, J. *Inorg. Chem.* **1981**, *20*, 2834.
(5) Korybut-Daszkiewicz, B.; Kojima, M.; Cameron, J. H.; Herron, N.; Chavan, M. Y.; Jircitano, A. J.; Coltrain, B. K.; Neer, G. L.; Alcock, N. W.; Busch, D. H. *Inorg. Chem.* **1984**, *23*, 903.
(6) (a) Alcock, N. W.; Lin, W.-K.; Jircitano, A.; Mokren, J. D.; Cornfield, P. W. R.; Johnson, G.; Novotnak, G.; Cairns, C.; Busch, D. H. *Inorg. Chem.* **1987**, *26*, 440. (b) Stevens, J. C.; Jackson, P. J.; Schammel, W. P.; Christoph, G. G.; Busch, D. H. *J. Am. Chem. Soc.* **1980**, *102*, 3283.
(7) (a) Traylor, T. G.; Traylor, P. S. *Annu. Rev. Biophys. Bioeng.* **1982**, *11*, 105. (b) Collman, J. P.; Halbert, T. R.; Suslick, K. S. *Metal Ion Activation of Dioxygen*; Spiro, T. G., Ed.; John Wiley & Sons: New York, 1980.
(8) (a) Niederhoffer, E. C.; Timmons, J. H.; Martell, A. E. *Chem. Rev.* **1984**, *84*, 137. (b) Jones, R. D.; Summerville, D. A.; Basolo, F. *Chem. Rev.* **1979**, *79*, 139.
(9) Stevens, J. C.; Busch, D. H. *J. Am. Chem. Soc.* **1980**, *102*, 3285.
(10) Stevens, J. C. Ph.D. Dissertation, The Ohio State University, 1979.
(11) Jackson, P. Ph.D. Dissertation, The Ohio State University, 1981.
(12) Perrin, D. D.; Armarego, W. L. F.; Perrin, D.R. *Purification of Laboratory Chemicals*, 2nd ed.; Pergamon Press: Oxford, England, 1980.
(13) Cairns, C. J.; Busch, D. H. *Inorg. Synth.*, in press.
(14) Busch, D. H.; Olszanski, D. J.; Stevens, J. C.; Schammel, W. P.; Kojima, M.; Herron, N.; Zimmer, L. L.; Holter, K. A.; Mocak, J. *J. Am. Chem. Soc.* **1981**, *103*, 1472.
(15) Gagné, R. R.; Koval, C. A.; Lisensky, G. C. *Inorg. Chem.* **1980**, *19*, 2855.

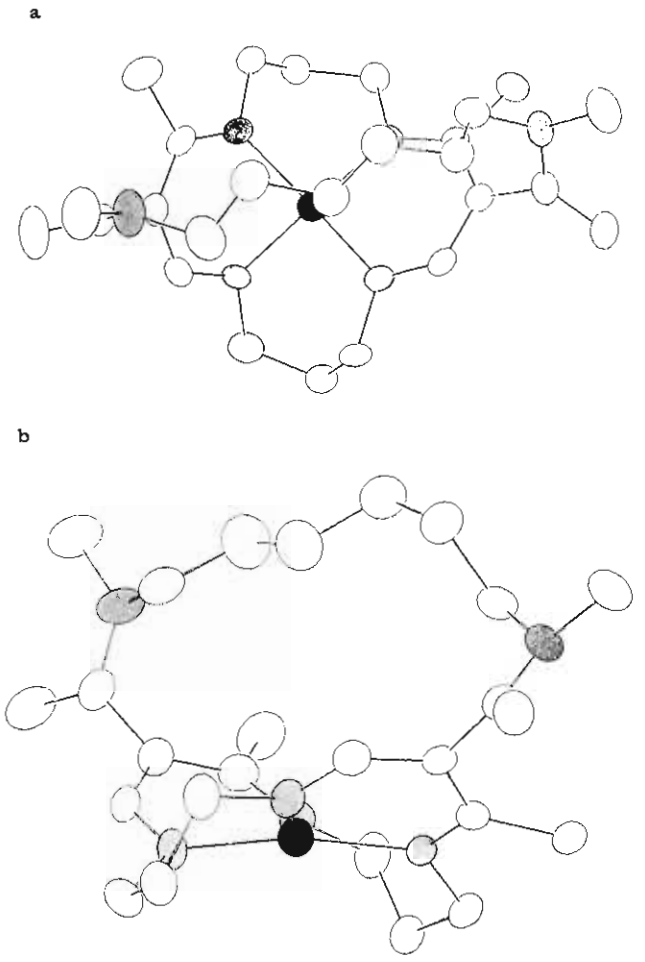

Figure 1. Structure of [Co{$(CH_2)_2(MeN)_2(CH_2)$6[16]cyclidene}]: (a) view from above, showing twisting of the "vinyl" groups and the positioning of the bridge above the metal atom; (b) view into the cavity.

to-scan ratio of 0.5 at the beginning and end of each 2θ scan. A total of 5832 reflections (4435 unique and 2666 with $I > 3\sigma_I$) were collected and used in structural determination. Intensities and standard deviations were calculated according to the formula $I = r(S - RB)$ and $\sigma_I = [r(S + R^2B)]^{1/2}$, respectively, where r is the scan rate in degrees/minute, S is the total scan count, R is the scan-to-background time ratio, and B is the total background count. Six standard reflections monitored every 100 reflections showed only random fluctuations over a 0.0034 range. The data were corrected for background, and Lorentz and polarization factors were applied to obtain structure factors. An absorption correction was not made. Wilson's method was used to bring F^2 to a relatively absolute scale. The σ_I^2 values were scaled by increasing the σ_I^2 values obtained from counting statistics by $P\sigma_I^2$, where P was chosen as the root-mean-square deviation of the standard reflections.

Solution and Refinement of Structures. The position of the heavy atom was ascertained from a Patterson map, and the positions of the remaining nonhydrogen atoms were revealed by subsequent Fourier maps. Refinement was performed by using full-matrix least-squares techniques, during which the function $\sum(w(|F_o| - |F_c|))^2$ was minimized. The data were weighted according to $1/\sigma(F)^2$. Residuals were calculated as $R = \sum(|F_o| - |F_c|)/\sum|F_o|$ and $R_w = \sum w(|F_o| - |F_c|)^2/\sum w|F_o|^2)^{1/2}$. Atomic scattering factors were taken from ref 16 for H, C_{cov}, N, and Co. All calculations were carried out on an Amdahl 470/V6 computer in the Computer Center of The Ohio State University with the CRYM[17a] and XRAY72[17b] crystallographic computing systems. Isotropic refinement resulted in convergence at $R = 0.095$. At this point the thermal parameters were allowed to vary anisotropically. Hydrogen atom positions were calculated, and hydrogen atoms were introduced as fixed contributions. Subsequent full-matrix least-squares refinement resulted in convergence at $R = 0.064$ and $R_w = 0.073$. In the final cycle of refinement, no atom shifted by more than 0.05 of its esd. A final difference map was featureless.

(16) *International Tables for X-ray Crystallography*; Kynoch Press: Birmingham, England, 1974; Vol IV.

(17) (a) DuChamp, D. J. *Program and Abstracts*; American Crystallographic Association Meeting, Bozeman, MT, 1964; Paper B14. As modified by G. G. Christoph, while at The Ohio State University. (b) Technical Report TR-192; Computer Science Center, University of Maryland: College Park, MD, 1972.

Scheme I

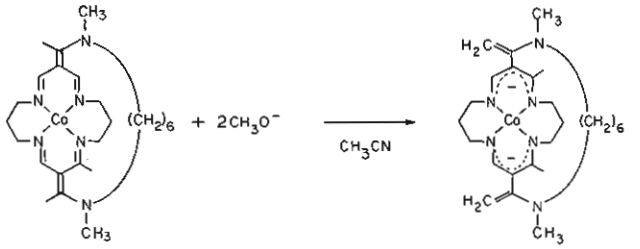

Table II. Atomic Coordinates for [Co{$(CH_2)_2(MeN)_2(CH_2)_6$[16]cyclidene(2−)}]

atom	*x*	*y*	*z*
Co	0.66796 (7)	0.42008 (9)	0.44086 (6)
N1	0.6112 (4)	0.3650 (5)	0.3272 (3)
N2	0.7751 (4)	0.5036 (5)	0.4209 (3)
N3	0.7584 (4)	0.4087 (5)	0.5550 (3)
N4	0.5473 (4)	0.3658 (4)	0.4595 (3)
N5	0.8877 (5)	0.2028 (6)	0.3221 (4)
N6	0.6139 (4)	0.0788 (5)	0.6181 (3)
C1	0.6725 (5)	0.3316 (6)	0.2915 (4)
C2	0.7777 (5)	0.3691 (6)	0.3181 (4)
C3	0.8173 (5)	0.4617 (6)	0.3740 (4)
C4	0.8270 (6)	0.6080 (6)	0.4697 (4)
C5	0.8489 (5)	0.5943 (6)	0.5595 (4)
C6	0.8629 (5)	0.4672 (7)	0.5867 (4)
C7	0.7418 (5)	0.3342 (6)	0.6050 (4)
C8	0.6471 (5)	0.2807 (5)	0.5930 (4)
C9	0.5495 (5)	0.3096 (5)	0.5244 (4)
C10	0.4385 (5)	0.3960 (6)	0.3956 (4)
C11	0.4411 (5)	0.4389 (6)	0.3167 (4)
C12	0.4958 (5)	0.3511 (7)	0.2840 (4)
C13	0.6256 (6)	0.2510 (8)	0.2166 (5)
C14	0.4478 (5)	0.2813 (6)	0.5341 (4)
C15	0.8524 (5)	0.3125 (7)	0.2883 (4)
C16	0.8812 (7)	0.3605 (9)	0.2345 (5)
C17	0.9494 (8)	0.1340 (9)	0.2909 (6)
C18	0.6481 (5)	0.1891 (6)	0.6530 (4)
C19	0.6733 (6)	0.2166 (7)	0.7321 (4)
C20	0.6010 (7)	−0.0128 (7)	0.6691 (5)
C21	0.9049 (7)	0.1772 (8)	0.4096 (6)
C22	0.8450 (7)	0.0733 (8)	0.4160 (5)
C23	0.8358 (7)	0.0693 (8)	0.4977 (5)
C24	0.7831 (6)	−0.0368 (8)	0.5116 (5)
C25	0.7521 (6)	−0.0202 (7)	0.5823 (4)
C26	0.6429 (5)	0.0382 (6)	0.5537 (4)

Results and Discussion

Synthesis. The parent C_6-bridged complexes were deprotonated by the reaction with 2 equiv of sodium methoxide, as shown in Scheme I. The deeply colored neutral complexes, [Ni{$(CH_2)_2(MeN)_2(CH_2)_6$[16]cyclidene}] and [Co{$(CH_2)_2(MeN)_2(CH_2)_6$[16]cyclidene}], are soluble in nonpolar solvents such as benzene, toluene, and chloroform. The deprotonated complexes can be reprotonated in organic solvents by the addition of acid. In fact, the crystal structure of [Co{$(CH_3)_2(MeN)_2(CH_2)_6$[16]cyclidene}]$(PF_6)_2$ was determined with crystals grown from a methanolic benzene solution of [Co{$(CH_2)_2(MeN)_2(CH_2)_6$[16]cyclidene}] that had been reprotonated with *p*-toluic acid.[10]

Crystal Structure. Figures 1 and 2 show the molecular structure and labeling scheme for the complex [Co{$(CH_2)_2(MeN)_2(CH_2)_6$[16]cyclidene}]. Final atomic position coordinates are given in Table II. The individual bond lengths and bond angles are unremarkable. Selected bond lengths are given in Table III, along with the analogous bond lengths for the parent protonated cobalt(II) cyclidene complex for purposes of comparison.

The changes in bond lengths accompanying deprotonation of the C_6-bridged cobalt(II) complex can be understood in terms of

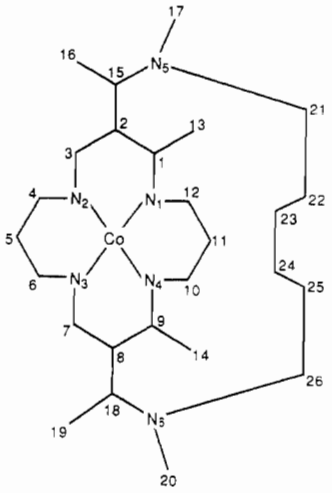

Figure 2. Numbering used in Tables II and III (crystallographic data).

Table III. Selected Bond Lengths for the Complexes (A) $[Co\{(CH_3)_2(MeN)_2(CH_2)_6[16]cyclidene\}]$ and (B) $[Co\{(CH_3)_2(MeN)_2(CH_2)_6[16]cyclidene\}](PF_6)_2$ and Individual and Average Differences

bond	d(A), Å	d(B), Å	d(A) − d(B), Å	(d(A) − d(B))$_{av}$, Å
Co–N1	1.942 (10)	1.89	0.05	0.03
Co–N4	1.935 (6)	1.93	0.01	
Co–N2	1.916 (7)	1.93	−0.01	−0.01
Co–N3	1.888 (14)	1.90	−0.01	
C1–N1	1.314 (11)	1.31	0.00	0.00
C9–N4	1.312 (9)	1.32	−0.01	
C1–C2	1.391 (11)	1.51	−0.12	−0.07
C8–C9	1.422 (14)	1.45	−0.03	
C2–C3	1.391 (10)	1.50	−0.11	−0.08
C7–C8	1.375 (10)	1.43	−0.06	
C3–N2	1.297 (11)	1.25	0.05	0.03
C7–N3	1.319 (10)	1.31	0.01	
C2–C15	1.494 (12)	1.41	0.08	0.07
C8–C18	1.487 (10)	1.44	0.05	
C15–C16	1.304 (14)	1.52	−0.22	−0.23
C18–C19	1.340 (11)	1.54	−0.24	
C15–N5	1.381 (10)	1.35	0.03	0.04
C18–N6	1.389 (9)	1.34	0.05	

the resonance structures that describe the π bonding in these complexes. For the parent complex, the principal resonance structure will be the structure V, although contributions from

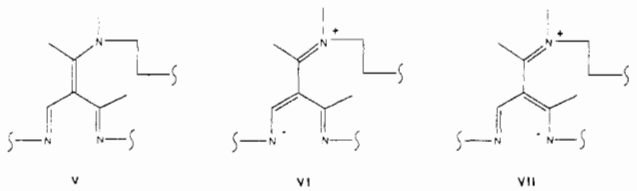

V VI VII

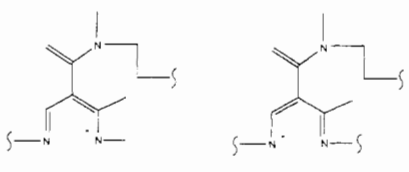

VIII IX

structures VI and VII may be expected.[4] For the deprotonated complex, one can expect significant contributions from both structures VIII and IX. According to these resonance structures,

Table IV. Cyclic Voltammetry Data[a] for the Parent and Deprotonated Lacunar Complexes

	potential, V vs $Fc^{+/0}$	
	M = Ni	M = Co
$[M\{(CH_3)_2(MeN)_2(CH_2)_6[16]cyclidene\}]^{3+/2+}$	0.76[b]	0.31[b]
$[M\{(CH_2)_2(MeN)_2(CH_2)_6[16]cyclidene\}]^{+/0}$	−0.23[c]	−0.42[c]

[a] Measured at a platinum disk electrode in 0.2 M TBAT/CH_2Cl_2 at 100 mV/s. Potentials reported vs the ferrocenium/ferrocene couple. [b] Reversible couple; $E_{1/2}$ reported. [c] Irreversible; $E_{p,a}$ reported.

deprotonation should lead to roughly the following changes in bond order (labels according to Figure 2): C1–N1, 2 to 1.5; C1–C2, 1 to 1.5; C2–C3, 1 to 1.5; C3–N2, 2 to 1.5; C2–C15, 2 to 1; C15–C16, 1 to 2. Furthermore, these changes should be reflected in the differences in bond lengths between the two structures.

Examination of the data in Table III shows that the differences in bond length upon deprotonation are in agreement with the changes in bond order predicted from the resonance structures. The greatest difference is observed for the vinyl methyl carbon, which shows an average decrease in bond length of 0.23 Å, consistent with double-bond formation upon deprotonation of that carbon. The C1–C2, C2–C3, and C2–C15 bond length changes are substantial and in the direction expected from the changes in bond order. The differences in bond length for C1–N1 and C3–N2 are not meaningful with respect to the esd's of the individual bond lengths. The similarity of these bond lengths for the deprotonated and parent complexes is not unexpected, given that bond lengths of bond order 1.5 are expected to lie between the single-bond and double-bond values but closer to the double-bond value.[18] In fact, the reason that the C1–C2, C2–C3, and C2–C15 bond lengths do not change by greater amounts is probably a result of the small, but finite, contributions to the protonated complex from resonance structures VI and VII. The involvement of these resonance structures would explain the slight lengthening of the C15–N5 bond upon deprotonation.

The changes in bond order in the conjugated portion of the macrocycle facilitate rotation at the points where the bridge is attached to the chelate ring in a manner not possible for the parent cyclidene complexes.[6a] This is clearly seen in Figure 1. The two attaching arms for the bridging hexamethylene group are oriented very differently. As displayed in Figure 1, the right-hand group has a familar orientation (refer to structure I), while the group on the left side is rotated by almost 90°. This produces a highly unsymmetrical cavity. However, the cavity dimensions are not unusual. The height of the cavity is measured by the vertical distances Co–C24 and Co–C23, and these are 5.41 and 4.50 Å, respectively. For comparison, the distances from the metal atom to the centers of the centermost C–C bonds in the structures of two hexamethylene-bridged species that are not deprotonated are 5.13 and 4.82 Å.[19] Similarly, the width of the cavity is not unusual with N5–N6 = 6.43 Å (literature, 6.74 and 6.94 Å) and C15–C18 = 8.24 Å (literature, 6.63 and 6.90 Å). The long C15–C18 distance arises from the unusual orientation of one of the risers, as mentioned above. The unusual dissymmetry in the risers facilitates the occurrence of an equally unusual conformation in which the first five of the six bridging methylene groups all approximate anti forms.[19] This is reflected by the torsion angles. Proceeding from the misoriented riser, these angles are 162.9, 176.0, and 165.40°. The next angle of 86.0° marks the termination of the excursion of this highly favorable conformation. The final torsional angle is also large, 168.8°.

Electrochemistry. In addition to allowing one to understand the structural changes associated with deprotonation of the cyclidene complexes, resonance structures VIII and IX suggest that deprotonation will result in a redistribution of electron density

(18) Pauling, L. *The Nature of the Chemical Bond*, 2nd ed.; Cornell University Press: Ithaca, NY, 1948.
(19) Alcock, N. W.; Lin, W.-K.; Cairns, C.; Pike, G. A.; Busch, D. H. *J. Am. Chem. Soc.*, in press.

with resulting increases in the vicinity of the metal center. The centralization of electron density and concomitant reduction in positive charge upon deprotonation are expected to make the cobalt(II) complex easier to oxidize, and this should be manifested in the electrochemistry of these complexes.

Electrochemical data for the parent and deprotonated cobalt(II) cyclidene complexes are given in Table IV, along with similar data for the analogous nickel(II) complexes. Dichloromethane was employed as the solvent in order to obtain reasonable solubility with the neutral deprotonated complexes. The parent cobalt(II) and nickel(II) complexes showed reversible couples in 0.1 M TBAT/CH_2Cl_2 at 0.31 and 0.76 V, respectively, vs $Fc^{+/0}$. On the basis of previous work in acetonitrile, these reversible one-electron waves can be assigned as the $M^{III/II}$ couples (M = Co, Ni),[3-5,20] although the ultimate nature of the oxidized complex involves a contribution from a ligand-oxidized state and depends on the cyclidene superstructure.[20] The observed 0.45-V difference between the redox couples is typical of this class of complexes. Both of the complexes gave adsorption waves at higher potentials (irreversible for cobalt, reversible for nickel), which may be assigned as ligand oxidations.[20] The adsorptive nature of the second waves is probably a result of forming tetracationic species in the nonpolar solvent, dichloromethane.

Deprotonation has a profound effect on the electrochemistry of the cobalt(II) and nickel(II) C_6-bridged complexes. The deprotonated cobalt(II) and nickel(II) complexes exhibit totally irreversible oxidation waves with peak potentials of –0.42 and –0.23 V, corresponding to cathodic shifts of roughly 0.7 and 1.0 V, respectively. The total irreversibility found for these complexes is reminiscent of that found for certain nickel(II) Schiff base complexes[21]—the common feature here being the dianionic ligands and overall neutral charge of the complexes. Both of the deprotonated cyclidene complexes show multiple oxidations following the first oxidation; however, the nature of these oxidations would be difficult to assign given the irreversible nature of the first process.

It is interesting that the difference between the peak potentials for the deprotonated complexes (0.19 V) is less than half that of the parent complexes (0.45 V). This may suggest that the nature of the redox process for the deprotonated cobalt(II) and nickel(II) complexes may be more similar than that of the parent complexes, possibly involving a greater contribution from ligand oxidation. If so, the irreversibility of the deprotonated complexes may involve ligand radical reactions.[20] An EC mechanism of this kind has been proposed for a nickel(II) macrocyclic complex.[22] In light of the rapid decomposition of the deprotonated complexes following oxidation, it will be difficult to design an experiment to test for the exact nature of the oxidized species.

Regardless of the precise nature of the oxidation products, the obvious effect of deprotonation is to make the cyclidene complexes much easier to oxidize, as expected from the increased electron density at the metal center and the reduction in charge. The increased electron density at the metal center might also be expected to affect the reactivity of the cobalt(II) complex with dioxygen.[23]

Reactions with Dioxygen. The parent macrocyclic complex [Co{$(CH_3)_2(MeN)_2(CH_2)_6$[16]cyclidene}]$(PF_6)_2$ is a well-characterized oxygen carrier[1b,9] with robust properties, including a substantial affinity at room temperature and reversible binding even in protonic solvents such as water. It has been pointed out that cyclidenes confer dioxygen affinities on metal ions a few orders of magnitude greater than those associated with porphyrin complexes. Further, the well-known correlation of O_2 affinity with electrode potential[23] suggests that the deprotonated cyclidene derivative should bind more strongly to O_2 than does the parent complex. While color changes support this expectation, the rapid oxidation of the deprotonated complex by O_2 has so far frustrated attempts to measure its dioxygen affinity. The autoxidation process is complicated, but the observed rates can be compared. The value of k_{OBS} for the new complex is 1.9×10^{-3} s^{-1} at 30 °C in 2 M *N*-MIm/CH_3CN in the presence of about 200 Torr of O_2, while the corresponding value for the parent complex is 9.6×10^{-5} s^{-1}.

Acknowledgment. We thank Wang Kan Lin for assistance in obtaining the crystallographic data and Air Products and Chemicals, Inc., for support of this research. The support of the National Science Foundation is also gratefully acknowledged.

Supplementary Material Available: Tables of crystal data, hydroen atom coordinates, temperature factors, bond distances, and bond angles (5 pages); a listing of structure factors (18 pages). Ordering information is given on any current masthead page.

(20) Chavan, M. Y.; Meade, T. J.; Busch, D. H.; Kuwana, T. *Inorg. Chem.* **1986**, *25*, 314.
(21) Goldsby, K. A.; Jircitano, A. J.; Minahan, D. M.; Ramprasad, D.; Busch, D. H. *Inorg. Chem.* **1987**, *26*, 2651.
(22) Bailey, C. L.; Bereman, D. D.; Rillema, D. R.; Nowak, R. *Inorg. Chem.* **1984**, *23*, 3956.
(23) (a) Carter, M. J.; Rillema, D. P.; Basolo, F. *J. Am. Chem. Soc.* **1974**, *96*, 392. (b) Carter, M. J.; Englehardt, L. M.; Rillema, D. P.; Basolo, F. *J. Chem. Soc., Chem. Commun.* **1973**, 810.